Struct Chem (2012) 23:1131–1142
DOI 10.1007/s11224-011-9934-5

ORIGINAL RESEARCH

X-ray crystal structures and conformational analysis of cyclic acetals derived from tartaric acid and rigid spacer units

Diana Eißmann · Felix Katzsch · Edwin Weber

Received: 31 August 2011 / Accepted: 16 December 2011 / Published online: 17 January 2012

Abstract Three tartaric ester and tartaric acid derivatives (**1**–**3**) with the hydroxy groups being linked via cyclic acetal (1,3-dioxolane) formation to a rigid core, containing phenyl and ethynyl units, have been synthesized. Their crystal structures are reported, emphasizing the molecular geometry, intermolecular interactions, and the resulting packing motifs. All dioxolane rings present in the crystal structures of **1**–**3** are analyzed and compared with regard to their conformational behavior. In spite of similar substitution patterns, the dioxolane units adopt different conformations including twist and varying envelope isomers. The crystal structures are dominated by C–H···O (esters **1** and **2**) and O–H···O (acid **3**) hydrogen bonds, leading to different types of packing motifs being characteristic of strand and layer formation.

Keywords Tartaric acid derivatives · Dioxolane · Conformational analysis · X-ray analysis · Hydrogen bonding

Introduction

Tartaric acid is one of the most important natural α-hydroxycarboxylic acids, being in the form of its sodium ammonium salt the first compound that was separated into its enantiomeric forms by Pasteur [1]. Furthermore, tartaric acid and its derivatives are known for their outstanding complexation properties [2] giving rise to numerous applications, especially in analytical fields such as a masking agent [3] or for the detection of reducing sugars [4]. In organic synthesis, tartrates are used as chiral auxiliaries, as resolving agents and for the synthesis of chiral building blocks. [5–7] Out of three possible stereoisomers, the natural L(+)-tartaric acid is the most common and is therefore readily available in its enantiopure form.

Molecules, the crystal structures of which are reported in this article, were designed in order to use them or their corresponding carboxylic acids as tectons for the formation of non-covalent organic frameworks (NoCOFs) or as linkers for metal organic framework (MOF) synthesis. [8, 9] Hence, molecular structures are supposed to contain a rigid core (phenyl and ethynyl units) as well as carboxylic acid functions in order to assemble via hydrogen bonding or to coordinate with metal ions. Following this line, chiral tartaric acid moieties attached to the phenyl ring of the rigid core by a transacetalization reaction, giving rise to a cyclic acetal (1,3-dioxolane), are promising molecular structures. While several tartaric acid and tartaric ester-derived dioxolanes with varying substitution patterns have been described in the literature [10–12], the compounds presently studied in this article have not been reported before.

Here, we present the synthesis and the results of X-ray crystal structure analyses of diethyl tartrate derivatives **1** and **2** as well as tartaric acid derivative **3** (Fig. 1) laying emphasis on the modes of crystal packing, types of intermolecular interactions and the molecular structures. Since all three compounds consist of one or two dioxolane moieties, it is quite obvious to make a comparison with regard to the conformational behavior including crystal structures of similar dioxolanes [13–16], which is also a subject of this study.

D. Eißmann · F. Katzsch · E. Weber (✉)
Institut für Organische Chemie, Technische Universität Bergakademie Freiberg, Leipziger Str. 29, 09596 Freiberg, Sachsen, Germany
e-mail: edwin.weber@chemie.tu-freiberg.de

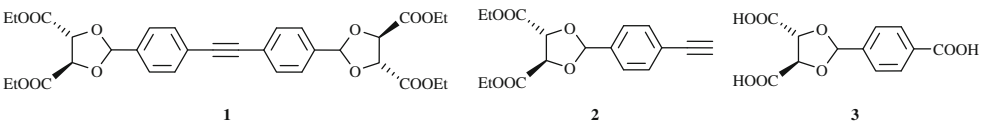

Fig. 1 Chemical structures of target molecules **1**, **2**, and **3**

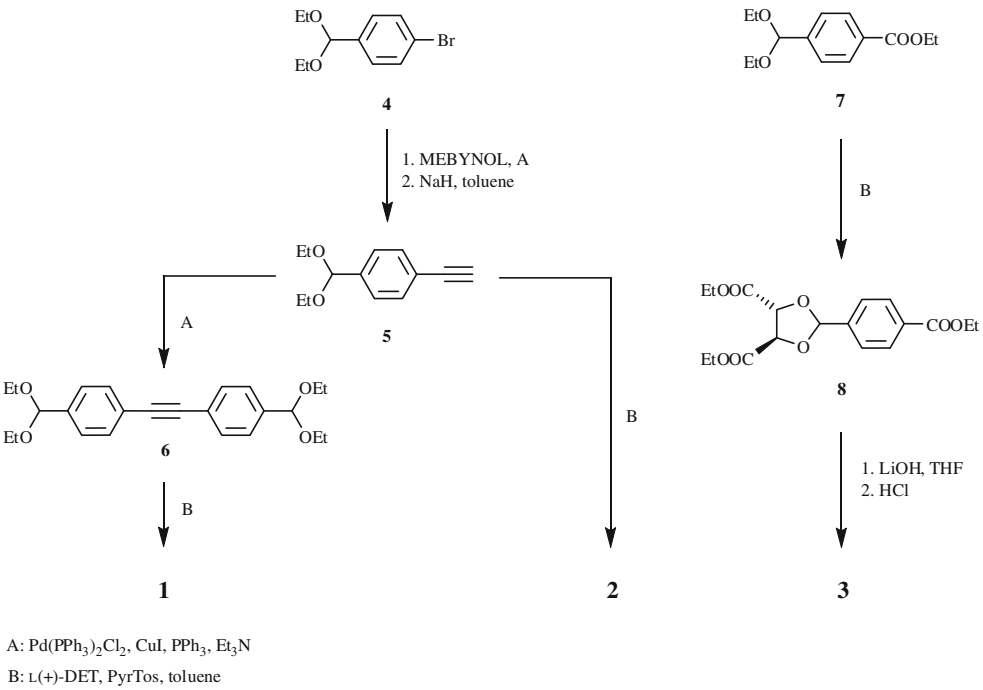

Fig. 2 Synthetic route to tartaric acid derivatives **1**, **2**, and **3**

Experimental

A summary of the synthetic routes of compounds **1**–**3** is given in Fig. 2.

General remarks

Melting points were measured on a BÜCHI Melting Point B-450 (BÜCHI Labortechnik AG, Flawil, Switzerland). ^{1}H NMR and ^{13}C NMR spectra (ppm) were recorded on a Bruker DPX 400 (400.1 and 100.6 MHz, respectively) and a Bruker Avance III 500 (500.1 and 125.8 MHz, respectively) using TMS as reference. IR spectra were obtained from a Nicolet FT-IR 510 spectrometer as liquid films in a NaCl cell or as KBr pellets. Optical rotation measurements were performed on a Perkin-Elmer 241 polarimeter at 20 °C and with $\lambda = 589.3$ nm (Na_D line). The $[\alpha]_D^{20}$ values are given in [deg mL dm^{-1} g^{-1}].

Commercial chemicals [*p*-bromobenzaldehyde diethylacetal (**4**), MEBYNOL, pyridinium tosylate] and solvents were used without further purification.

4-Ethynylbenzaldehyde diethylacetal (**5**)

4-Bromobenzaldehyde diethylacetal (**4**) (5.00 g, 19.3 mmol) and MEBYNOL (1.91 g, 22.7 mmol) were dissolved in degassed triethylamine (20 mL). To this solution, the catalyst [composed of $Pd(PPh_3)Cl_2$ (6.7 mg, 0.0095 mmol), CuI (6.5 mg, 0.034 mmol), and PPh_3 (12.5 mg, 0.048 mmol)] was added and the mixture was stirred at 110 °C under argon for 9 h. The suspension was diluted with diethyl ether and washed with aqueous NH_4Cl and NaCl solutions. After drying over Na_2SO_4, the solvent was removed under reduced pressure. The intermediate protected alkyne was obtained as a brownish-red liquid. For cleavage of the protecting group, toluene (p.a., 50 mL) and NaH (60% suspension in paraffin oil, 0.26 g, 2.6 mmol) were added and the mixture was refluxed for 16 h. Then dichloromethane (50 mL) was added and the mixture was filtered. The filtrate was washed with aqueous Na_2CO_3 and NaCl solutions. The organic layer was dried over Na_2SO_4 and the solvent removed under reduced pressure to yield 95% alkyne **4** as a brownish-red liquid. R_f (EtOAc/*n*-hexane 1:4) = 0.78. ^{1}H NMR ($CDCl_3$, 400.1 MHz) δ: 1.23 (t, $^{3}J_{HH} = 7.0$ Hz, 6H, CH_3); 3.07 (s, 1H, C≡CH); 3.56 (m, 4H, CH_2); 5.50 (s, 1H, CH); 7.43, 7.48 (2 d, $^{3}J_{HH} = 8.0$ Hz, 2H, aryl-H). ^{13}C NMR ($CDCl_3$, 100.6 MHz) δ: 15.1 (CH_3); 61.0 (CH_2); 77.3 (C≡CH); 83.5 (C≡CH); 100.9 (CH); 122.0, 126.6, 131.9, 139.8 (aryl-C). IR (liquid film, cm^{-1}) $\bar{\nu}$: 3289; 2978; 2931; 2879; 2359; 2109; 1925; 1706; 1608; 1565; 1445; 1392; 1337; 1211; 1174; 1115; 1094; 1054; 847; 816. GC–MS: $m/z = 204$ $[M]^+$.

4,4′-Bis(diethoxymethyl)tolane (**6**)

4-Bromobenzaldehyde diethylacetal (**4**) (19.02 g, 73.4 mmol), 4-ethynylbenzaldehyde diethylacetal (**5**) (15.00 g, 73.4 mmol), triethylamine (75 mL), $Pd(PPh_3)_2Cl_2$ (25.2 mg, 0.036 mmol), CuI (24.7 mg, 0.130 mmol), and PPh_3 (47.6 mg, 0.181 mmol) were reacted under the coupling conditions as given above and worked up correspondingly to obtain 31% of **6** as a colorless solid after recrystallization from ethanol/acetone (1:1). Mp. 72–74 °C. R_f (EtOAc/*n*-hexane 1:4) = 0.71. ^{1}H NMR ($CDCl_3$, 400.1 MHz) δ: 1.24 (t, $^3J_{HH}$ = 7.0 Hz, 12H, CH_3); 3.58 (m, 8H, CH_2); 5.52 (s, 2H, CH); 7.46, 7.52 (2 d, $^3J_{HH}$ = 8.4 Hz, 2H, aryl-H). ^{13}C NMR ($CDCl_3$, 100.6 MHz) δ: 15.2 (CH_3); 61.0 (CH_2); 89.4 (C≡C); 101.0 (CH); 123.1, 126.7, 131.4, 139.2 (aryl-C). IR (KBr, cm^{-1}) $\bar{\nu}$: 3053; 2971; 2923; 2908; 2873; 2363; 1932; 1717; 1613; 1565; 1518; 1483; 1451; 1442; 1388;1372; 1363; 1340; 1306; 1277; 1207; 1122; 1097; 1059; 1033; 1002; 960; 919; 875; 850; 805. GC–MS: *m/z* = 382 $[M]^+$.

Ethyl *p*-(diethoxymethyl)benzoic acid (**7**)

The compound was obtained in 91% yield as a yellow liquid by acetalization and esterification of 4-formylbenzoic acid with thionyl chloride and $HC(OEt)_3$ in ethanol according to the literature procedure [17]. R_f (EtOAc/*n*-hexane 1:4) = 0.65. Spectroscopic and other analytical data correspond to the literature specifications.

Tartaric acid derivatives **1**, **2**, and **8** (general procedure)

To a solution of the corresponding diethoxy acetal and L(+)-diethyl tartrate in toluene (p.a.), a catalytic amount of pyridinium tosylate was added. In order to remove the by-product ethanol from the mixture, the solvent was distilled off during the reaction. The residue was diluted with diethyl ether and washed with borax and water to remove unreacted L(+)-diethyl tartrate. After drying over Na_2SO_4, the solvent was removed under reduced pressure.

*2,2′-(Tolane-4,4′-diyl)bis[(4R,5R)-4,5-di(ethoxycarbonyl)-1,3-dioxolane] (**1**)*

4,4′-Bis(diethoxymethyl)tolane (**6**) (2.00 g, 5.2 mmol), L(+)-diethyl tartrate (2.37 g, 11.5 mmol), pyridinium tosylate (0.11 g, 0.4 mmol), and toluene (p.a., 100 mL) were used to yield 40% of **1** as a colorless solid after column chromatography (SiO_2, EtOAc/*n*-hexane 1:2). Mp 74–77 °C. R_f (EtOAc/*n*-hexane 1:2) = 0.31. $[\alpha]_D^{20}$ ($CHCl_3$, *c* = 0.01 mol L^{-1}) = +19.0. ^{1}H NMR ($CDCl_3$, 400.1 MHz) δ: 1.31 (m, 12H, CH_3); 4.31 (m, 8H, CH_2); 4.83, 4.95 (2 d, $^3J_{HH}$ = 4.0 Hz, 2H, CH); 6.17 (s, 2H, CH); 7.54–7.59 (m, 8H, aryl-H). ^{13}C NMR ($CDCl_3$, 100.6 MHz) δ: 14.1 (CH_3); 62.1 (CH_2); 77.4, 77.7 (CH); 89.8 (C≡C); 106.3 (CH); 124.7, 127.2, 131.6, 135.7 (aryl-C); 169.3 (C=O). IR (KBr, cm^{-1}) $\bar{\nu}$: 3066; 2987; 2933; 2898; 2873; 2360; 2224; 1761; 1742; 1613; 1562; 1521; 1439; 1416; 1401; 1369; 1350; 1302; 1255; 1220; 1195; 1100; 1036; 995; 960; 945; 850; 824. ESI–MS: *m/z* = 633.0 $[M+Na]^+$.

*2-(p-Ethynylphenyl)-(4R,5R)-4,5-di(ethoxycarbonyl)-1,3-dioxolane (**2**)*

p-Ethynylbenzaldehyde diethylacetal (**5**) (4.50 g, 0.025 mol), L(+)-diethyl tartrate (5.00 g, 0.027 mol), pyridinium tosylate (0.23 g, 1.0 mmol), and toluene (p.a., 180 mL) were used to yield 50% of **1** as a yellow oil after column chromatography (SiO_2, EtOAc/*n*-hexane 1:4) which crystallized on cooling to 0 °C. Mp. 55–59 °C. R_f (EtOAc/*n*-hexane 1:4) = 0.44. $[\alpha]_D^{20}$ ($CHCl_3$, *c* = 0.01 mol L^{-1}) = −7.2. ^{1}H NMR ($CDCl_3$, 500.1 MHz) δ: 1.30, 1.35 (2 t, $^3J_{HH}$ = 7.15 Hz, 3H, CH_3); 3.11 (s, 1H, CH); 4.27, 4.33 (2 t, $^3J_{HH}$ = 7.15 Hz, 2H, CH_2,); 4.83, 4.94 (2 d, $^3J_{HH}$ = 3.95 Hz, 1H, CH); 6.16 (s, 1H, CH); 7.51–7.56 (m, 4H, aryl-H). ^{13}C NMR ($CDCl_3$, 125.8 MHz) δ: 14.0, 14.1 (CH_3); 62.1, 62.1 (CH_2); 77.3, 77.7 (CH); 78.0, 83.2 (C≡C); 106.1 (CH); 123.7, 127.1, 132.1, 136.1 (aryl-C); 168.9, 169.5 (C=O). IR (KBr, cm^{-1}) $\bar{\nu}$: 3690; 3294; 3275; 3231; 3069; 2984; 2939; 2911; 2879; 2100; 1749; 1730; 1505; 1477; 1445; 1397; 1347; 1369; 1302; 1252; 1236; 1214; 1176; 1157; 1122; 1071; 1059; 1033; 979; 964; 951; 935; 865; 827; 764; 726. GC–MS: *m/z* = 317 $[M-H]^+$.

*2-[(p-Ethoxycarbonyl)phenyl]-(4R,5R)-4,5-di(ethoxycarbonyl)-1,3-dioxolane (**8**)*

Ethyl *p*-(diethoxymethyl)benzoic acid (**7**) (6.00 g, 23.8 mmol), L(+)-diethyl tartrate (5.40 g, 26.2 mmol), pyridinium tosylate (0.24 g, 0.99 mmol) and toluene (p.a., 200 mL) were used to yield 71% of **8** as a yellow oil after column chromatography (SiO_2, EtOAc/*n*-hexane 1:4). R_f (EtOAc/*n*-hexane 1:4) = 0.36. $[\alpha]_D^{20}$ ($CHCl_3$, c = 0.01 mol L^{-1}) = −10.1. ^{1}H NMR ($CDCl_3$, 500.1 MHz, ppm) δ: 1.30, 1.36, 1.40 (3 t, $^3J_{HH}$ = 7.15 Hz, 3H, CH_3); 4.26, 4.33, 4.38 (3 q, $^3J_{HH}$ = 7.15 Hz, 2H, CH_2); 4.85, 4.97 (2 d, $^3J_{HH}$ = 3.90 Hz, 1H, CH,); 6.21 (s, 1H, CH); 7.67, 8.07 (2 d, $^3J_{HH}$ = 8.20 Hz, $^3J_{HH}$ = 8.40 Hz, 2H, aryl-H). ^{13}C NMR ($CDCl_3$, 125.8 MHz, ppm) δ: 14.0, 14.1, 14.2 (CH_3); 61.0, 62.0, 62.0 (CH_2); 77.3, 77.6, 105.8 (CH); 127.0, 129.5, 131.7, 140.1 (aryl-C); 166.1, 168.8, 169.3 (COOEt). IR (liquid film, cm^{-1}) $\bar{\nu}$: 2984; 2941; 2907; 2873; 1756; 1719; 1617; 1580; 1513; 1470; 1445; 1430; 1393; 1365; 1279; 1214; 1174; 1103; 1020; 956; 857; 771; 706. GC–MS: *m/z* = 365 $[M-H]^+$.

*2-(p-Carboxyphenyl)-(4R,5R)-4,5-dicarboxyl-1,3-dioxolane (**3**)*

A solution of the ester **7** (0.50 g, 1.36 mmol) and LiOH (0.19 g, 8.19 mmol) in THF (25 mL) and H_2O (10 mL) was stirred at room temperature for 5 h. The reaction mixture was diluted with water, acidified with 1 M HCl and repeatedly extracted with diethyl ether. After washing the combined organic extracts with water and drying it over Na_2SO_4, the solvent was removed under reduced pressure. The obtained crude product was purified by stirring it in cold dichloromethane to yield 66% of **3** as a colorless solid. Mp. 203–206 °C (dec). $[\alpha]_D^{20}$ (EtOH, $c = 0.01$ mol L^{-1}) $= -20.6$. ^{1}H NMR (DMSO-d_6, 500.1 MHz) δ: 4.79, 4.94 (2 d, $^3J_{HH} =$ 4.00 Hz, $^3J_{HH} = 3.90$ Hz, 1H, CH); 6.08 (s, 1H, CH); 7.69, 7.99 (2 d, $^3J_{HH} = 8.15$ Hz, $^3J_{HH} = 8.10$ Hz, 2H, aryl-H); 13.63 (br s, 3H, COOH). ^{13}C NMR (DMSO-d_6, 125.8 MHz) δ: 76.9, 77.3, 104.5 (CH); 127.5, 129.3, 132.1, 140.7 (aryl-C); 167.0, 170.5, 171.0 (COOH). IR (KBr, cm^{-1}) $\bar{\nu}$: 3120; 2670; 2550; 1755; 1685; 1581; 1515; 1426; 1391; 1223; 1100; 1043; 1017; 986; 951; 881; 856; 789; 770; 729 ESI–MS: $m/z = 281.03$ $[M-H]^-$.

Crystal structure determination

Crystals of **1**–**3** suitable for X-ray analysis were obtained by slowly cooling a hot solution of **1** in EtOH, cooling the oily sample of **2** to 0 °C and slowly evaporating a solution of **3** in Et_2O/THF (1:1).

The X-ray diffraction intensities were recorded on a Bruker Kappa diffractometer equipped with an APEX II CCD area detector and graphite-monochromatized MoK_α radiation ($\lambda = 0.71073$ Å) employing φ and ω scan modes. The data were corrected for Lorentz and polarization effects. The SAINT program [18] was utilized for integration of the diffraction profiles. For compound **3** (anisotropic crystal shape), a semiempirical absorption correction was applied using the SADABS program [19]. The crystal structures were solved by direct methods and refined by full-matrix least-squares refinement against F^2 using SHELXL-97 [20]. All non-hydrogen atoms were refined anisotropically; hydrogen atoms were generated at ideal geometrical positions and refined with the appropriate riding model or positioned by difference Fourier synthesis. Because of the high uncertainty of the absolute parameter x (FLACK) [21, 22] in the CIF file, the final refinement steps of **1**–**3** were carried out by using the MERG 4 option in SHELXL-97. The absolute configuration at the asymmetry centers of the products is determined by the chirality of the used stereoisomer of tartaric acid. So the molecules have (*R*)-configuration at all chirality centers [C(9), C(10), C(25), C(26) in **1**, C(9), C(10), C(9A), C(10A) in **2** and C(9), C(10) in **3**]. Geometrical calculations were performed using PLATON [23] and molecular graphics were generated using SHELXTL [20].

Results and discussion

The crystals of **1** and **2** were found to be free of solvent, while **3** was analyzed to contain water in a 1:1 (**3**:H_2O) stoichiometric ratio enclosed in the crystal. Crystal data and details of the structure refinement are summarized in Table 1. Geometric parameters of intermolecular interactions of the compounds studied are listed in Table 2, while Table 3 summarizes selected interplanar angles in the crystal structure of compound **2**. A conformational comparison of the dioxolane moieties in compounds **1**–**3** and in similar derivatives described in the literature [13–16] is given in Tables 4 and 5. Figure 3 shows the molecular structures (ellipsoid plots) with atom labelling schemes, while packing illustrations and specific patterns of intermolecular contacts are given in Figs. 4, 5, 6, and 7.

Crystal structure of tartaric ester **1**

The compound crystallizes as colorless needles in the monoclinic space group $P2_1$ with one molecule of **1** in the asymmetric unit (Fig. 3). The packing is predominantly stabilized by weak C–H···O [24, 25] and C–H···π contacts [26, 27]. With the dioxolane moiety as the hydrogen donor and the carbonyl oxygen atom as the acceptor, molecules are forced into chains (A and B) along the b axis with a parallel alignment regarding the [503]-plane (Fig. 4). The interplanar twist angle between the phenyl rings of both chains is 58.3°, and between the phenyl rings and the [503]-plane, the interplanar angels are 29.4° and 31.4° (chains A and B, respectively). As illustrated in Fig. 4b, adjacent chains are linked by an inverse bifurcated C–H···O contact between a phenyl ring (hydrogen donor) and dioxolane as well as carbonyl moieties (hydrogen acceptors). Weak C–H···π contacts can be observed with aryl or ethyl groups as hydrogen donors. Moreover, strands which show an ABAB-alignment of adjacent chains are connected by C–H···O contacts between two ester moieties.

Crystal structure of tartaric ester **2**

By cooling an oily sample of **2** to about 0 °C, colorless crystals, showing the monoclinic space group $P2_1$ with two molecules of **2** in the asymmetric unit (Fig. 3), were obtained. The packing of molecules 1 (C1–C17, O1–6) and 2 (C1A–C17A, O1A–6A) can be described as layers parallel to the [101]-plane with an ABA′B′-pattern. Layers A and A′ both consist of type 1 molecules, which are aligned

Table 1 Crystallographic data for the compounds studied

Compound	**1**	**2**	**3**·H_2O
Empirical formula	$C_{32}H_{34}O_{12}$	$C_{17}H_{18}O_6$	$C_{12}H_{10}O_8 \cdot H_2O$
Formula weight (g mol^{-1})	610.59	318.31	300.22
Temperature (K)	153(2)	153(2)	153(2)
Wavelength (Å)	0.71073	0.71073	0.71073
Crystal system, space group	Monoclinic, $P2_1$	Monoclinic, $P2_1$	Monoclinic, $P2_1$
Unit cell dimensions			
a (Å)	15.7607(9)	8.2434(2)	4.7386(1)
b (Å)	5.5507(4)	15.9061(4)	11.0661(3)
c (Å)	17.8716(11)	12.4178(3)	12.2429(3)
α (°)	90	90	90
β (°)	108.528(3)	104.349(1)	91.705(2)
γ (°)	90	90	90
V ($Å^3$)	1482.42(16)	1577.43(7)	641.71(3)
Z	2	4	2
Calculated density (g cm^{-3})	1.368	1.340	1.554
Absorption coefficient (mm^{-1})	0.105	0.102	0.137
F(000)	644	672	312
Crystal size (mm^3)	0.34 × 0.06 × 0.02	0.50 × 0.23 × 0.18	0.30 × 0.30 × 0.04
θ Range for data collection (°)	2.08–27.50	2.12–27.50	2.48–30.00
Limiting indices	$-20 \le h \le 20$	$-10 \le h \le 10$	$-6 \le h \le 6$
	$-6 \le k \le 7$	$-20 \le k \le 20$	$-15 \le k \le 15$
	$-23 \le l \le 23$	$-16 \le l \le 16$	$-17 \le l \le 17$
Reflections collected/unique	30120/3767	30539/3754	16395/1959
	[R(int) = 0.0599]	[R(int) = 0.0350]	[R(int) = 0.0243]
Completeness to θ (%)	99.9	99.9	99.9
Data/restraints/parameters	3767/0/401	3754/1/419	1959/1/204
Goodness-of-fit on F^2	1.018	1.041	1.066
R indices [$I > 2\sigma(I)$]	$R_1 = 0.0413$,	$R_1 = 0.0296$,	$R_1 = 0.0283$,
	w$R_2 = 0.0813$	w$R_2 = 0.0726$	w$R_2 = 0.0744$
R indices (all data)	$R_1 = 0.0643$,	$R_1 = 0.0326$,	$R_1 = 0.0325$,
	w$R_2 = 0.0881$	w$R_2 = 0.0742$	w$R_2 = 0.0768$
$\Delta\rho_{max}/\Delta\rho_{min}$ (e $Å^{-3}$)	0.468/−0.274	0.214/−0.223	0.310/−0.162

in opposite directions. In the same way, layers B and B′ are formed by molecules of type 2. Interplanar angles involving the aromatic units facing one another and also the [101]-plane are summarized in Table 3. Similar to the crystal structure of **1**, the packing of **2** is stabilized by C–H···O and C–H···π contacts. Within one layer of molecules, the terminal alkyne group serves as a hydrogen bond donor [28] and the carbonyl oxygen as the corresponding acceptor site (Fig. 5). Furthermore, C–H···π contacts between ethyl hydrogen atoms and the π-system of alkyne moieties can be observed. Intermolecular contacts between dioxolane units (donor) and carbonyl oxygen atoms (acceptor) as well as between two edge-to-face assembled phenyl rings [29] connect layers A and B. The linkage between layers A and B′ is formed by C–H···O (donor: phenyl and dioxolane, acceptor: carbonyl) and C–H···π contacts (donor: phenyl, acceptor: alkyne). With dioxolane being both hydrogen donor and acceptor, interactions between layers A′ and B are formed. While the alkyne moiety is involved in several intermolecular contacts in the crystal structure of **2**, no similar interactions have been observed in the packing of compound **1**.

Crystal structure of tartaric acid derivative **3**

Compound **3** crystallizes as a monohydrate in the monoclinic space group $P2_1$ with one molecule of **3** and one water molecule in the asymmetric unit (Fig. 3). Molecules are arranged in wavelike layers extending parallel to the [102]-plane with an inclination angle of

Table 2 Geometric parameters of intermolecular interactions of the compounds studied

Compounds	Atoms involved	Symmetry	Distance (Å)		Angle (°)
			D···A	H···A	D–H···A
1	C3–H3···O11	$-x, 1/2 + y, 1 - z$	3.557(3)	2.68	153
	C7–H7···O1	$-x, -1/2 + y, -z$	3.402(3)	2.66	135
	C7–H7···O3	$-x, -1/2 + y, -z$	3.489(3)	2.60	156
	C10–H10···O5	$x, 1 + y, z$	3.311(4)	2.51	137
	C15–H15B···O6	$1 - x, -1/2 + y, -z$	3.560(3)	2.62	158
	C14–H14C···O10	$-x, -1/2 + y, -z$	3.560(4)	2.59	170
	C26–H26···O9	$x, -1 + y, z$	3.029(3)	2.56	108
	C29–H29B···O9	$-1 - x, -1/2 + y, 1 - z$	3.439(3)	2.68	134
	C6–H6···Cg1[a]	$-x, -1/2 + y, -z$	3.726(7)	3.00	135
	C13–H13B···Cg2[a]	$-x, -1/2 + y, -z$	3.559(7)	2.73	141
	C20–H20···Cg2[a]	$-x, 1/2 + y, 1 - z$	3.450(8)	2.71	135
	C31–H31B···Cg1[a]	$-x, 1/2 + y, 1 - z$	3.593(6)	2.75	143
2	C17–H17···O3	$2 - x, -1/2 + y, 1 - z$	3.246(2)	2.30	171
	C17A–H17B···O3A	$2 - x, -1/2 + y, 2 - z$	3.252(2)	2.33	164
	C4–H4···O3A	$2 - x, -1/2 + y, 2 - z$	3.305(2)	2.37	167
	C9A–H9A···O5	$x, -1 + y, z$	3.347(2)	2.36	170
	C10–H10···O5A	$1 - x, 1/2 + y, 2 - z$	3.244(2)	2.50	131
	C10A–H10A···O1	$2 - x, 1/2 + y, 2 - z$	3.155(2)	2.43	129
	C13–H13A···O3A	$x, 1 + y, z$	3.424(2)	2.53	150
	C3–H3···Cg2[b]	$2 - x, 1/2 + y, 2 - z$	3.710(8)	2.85	151
	C4A–H4A···Cg3[b]	$2 - x, -1/2 + y, 1 - z$	3.696(6)	2.82	154
	C15–H15A···Cg1[b]	$2 - x, 1/2 + y, 2 - z$	3.588(2)	2.87	130
	C15–H15D···Cg2[b]	$2 - x, -1/2 + y, 1 - z$	3.784(3)	2.83	163
3	O1G–H1G···O7	$2 - x, -1/2 + y, 1 - z$	2.808(2)	1.93(5)	161(4)
	O1G–H2G···O7	$2 - x, -1/2 + y, 2 - z$	2.996(2)	2.20(4)	160(4)
	O8–H8A···O2	$2 - x, -1/2 + y, 2 - z$	2.874(2)	2.59	101
	O8–H8A···O5	$x, -1 + y, z$	2.705(2)	1.87	173
	O4–H4···O1G	$1 - x, 1/2 + y, 2 - z$	2.557(2)	1.75(4)	163(3)
	O6–H6A···O3	$2 - x, 1/2 + y, 2 - z$	2.598(2)	1.77	167
	C9–H9···O2	$x, 1 + y, z$	3.249(2)	2.29	160
	C10-H10···O1G	$2 - x, -1/2 + y, 1 - z$	3.225(2)	2.39	141

[a] Cg1, centroids of atoms C2–C7 (phenyl); Cg2, centroids of atoms C18–C23 (phenyl)

[b] Cg1, centroids of atoms C1, C17 (alkyne); Cg2, centroids of atoms C1A, C17A (alkyne); Cg3, centroids of atoms C2–C7 (phenyl)

Table 3 Interplanar angles (°) between phenyl units of layers A, B, A′, B′ and the [010]-plane

A/[010]	A′/[010]	B/[010]	B′/[010]	A/A′	B/B′	A/B	A/B′
56.9	56.9	50.3	50.3	66.3	79.3	73.0	8.2

23.5° between the aromatic rings of adjacent molecules (Fig. 6). In contrast to the crystal structures of compounds **1** and **2**, the packing of **3** is stabilized by strong O–H···O hydrogen bonds. Within the molecular layer, interactions between two carboxylic moieties can be observed. However, no carboxylic acid dimers [30–32], being a strong supra-molecular synthon [33, 34], is formed although the carboxylic acid groups serve as hydrogen bond donor and acceptor sites. On the contrary, the crystal water can be regarded as a linkage element, supporting the stability of the crystal structure by forming strong O–H···O hydrogen bonds and weaker C–H···O contacts. This leads to an assembly of three molecules of **3** and two water molecules, giving rise to a cyclic hydrogen bond motif which is illustrated in Fig. 7.

Conformational analysis of the molecular structures of **1**, **2,** and **3**

As the tartaric acid derivative **1** features two independent dioxolane units, attached to a tolane spacer, and the asymmetric unit of **2** contains two non-equivalent molecules, there are five dioxolane moieties whose conformational features in the solid state can be compared.

Table 4 Conformational comparison of **1**, **2**, and **3** with similar dioxolane derivatives described in the literature (CSD acronyms)

Compound (CSD acronym)	Substitution pattern 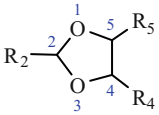		Pucker parameter (CP)		Conformation (Atoms out of plane)
			Q	*φ*	
1	R_2 = R′tolanyl	*trans*	0.383(3)	194.7(4)	Twist
	R_4 = COOEt		0.376(3)	207.0(4)	Envelope (C, position 2)
	R_5 = COOEt				
2	R_2 = *p*-ethynylphenyl	*trans*	0.355(2)	289.8(3)	Envelope (C, position 4)
	R_4 = COOEt		0.315(2)	291.9(3)	Envelope (C, position 4)
	R_5 = COOEt				
3	R_2 = carboxyphenyl	*trans*	0.354(2)	217.4(2)	Envelope (C, position 2)
	R_4 = COOH				
	R_5 = COOH				
DUDFOY [40]	R_2 = *m*-methoxyphenyl	*trans*	0.308(3)	165.5(6)	Twist
	R_4 = $CONH_2$				
	R_5 = $CONH_2$				
FOWZEX [41]	R_2 = *p*-chlorophenyl	*trans*	0.353(3)	50.8(5)	Twist
	R_4 = $CONH_2$				
	R_5 = $CONH_2$				
VOJGAD [13]	R_2 = *o*-fluorophenyl	*trans*	0.376(5)	24.8(8)	Twist
	R_4 = $CONH_2$				
	R_5 = $CONH_2$				
VOQLIX [14]	R_2 = *o*-bromophenyl	*trans*	0.335(10)	206.0(18)	Twist
	R_4 = $CONH_2$		0.395(10)	44.3(14)	Envelope (C, position 2)
	R_5 = $CONH_2$				
WEGXOW [15]	R_2 = dibenzofurane	*trans*	0.409(5)	212.0(7)	Envelope (C, position 2)
	R_4 = COO-*i*-Pr		0.220(5)	214.3(14)	Envelope (C, position 2)
	R_5 = COO-*i*-Pr				
XEYSEA [16]	R_2 = phenyl	*trans*	0.386(6)	59.2(9)	Twist
	R_4 = COOEt		0.290(6)	177.2(11)	Envelope (O, position 1)
	R_5 = COOEt				

Table 5 Interplanar angles (°) between mean planes of dioxolane rings (A) and adjacent phenyl moieties (B)

Compound	Plane A (atoms involved)	Plane B (atoms involved)	Interplanar angle (°) A/B
1			
(dioxolane 1)	(O1, O2, C8–C10)	(C2–C7)	72.7
(dioxolane 2)	(O7, O8, C24–C26)	(C18–C23)	27.2
2			
(molecule 1)	(O1, O2, C8–C10)	(C2–C7)	54.3
(molecule 2)	(O1A, O2A, C8A–C10A)	(C2A–C7A)	45.2
3	(O1, O2, C8–C10)	(C2–C7)	70.9

The dioxolane conformation is described by applying the pucker parameters according to Cremer and Pople [35], which were obtained using the crystallographic program PLATON [23]. A graphical summary of the parameters and the resulting conformations is given with the help of a so-called pseudorotation wheel (deduced from the pseudorotation wheels of cyclopentane [36, 37] and furanose [38]) in Fig. 8. Although the substitution pattern of the dioxolane ring is similar in all five cases, molecules of compounds **1**, **2**, and **3** show significant conformational

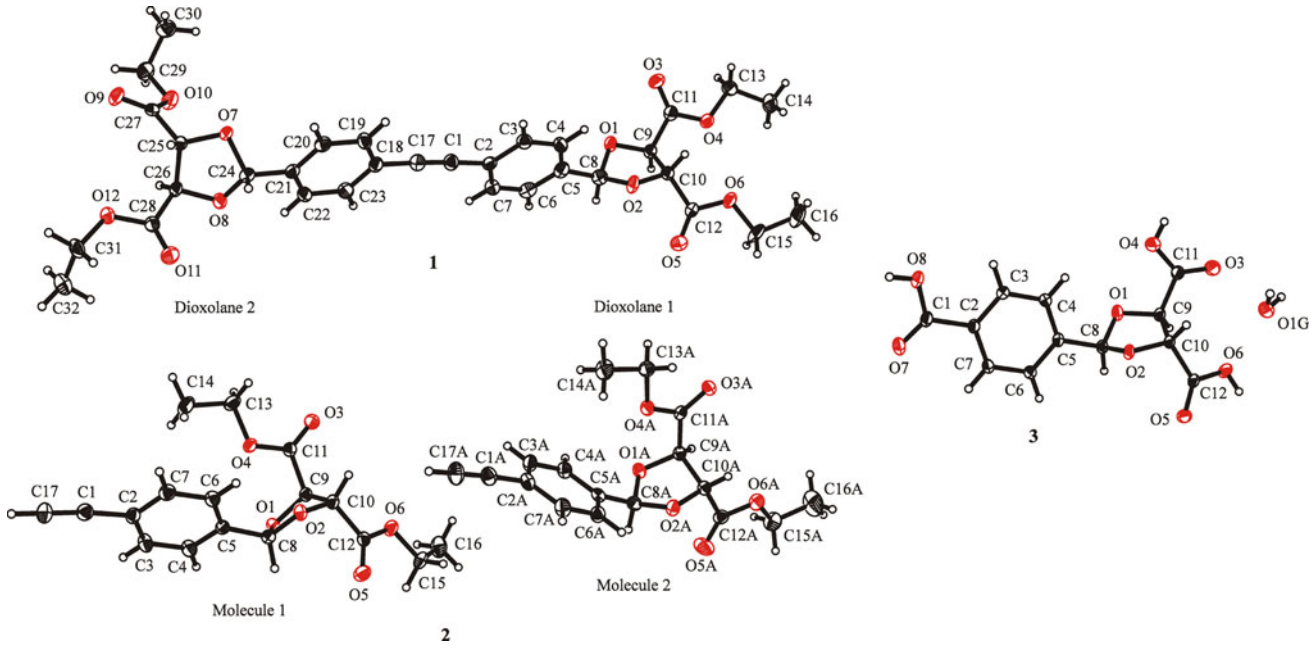

Fig. 3 Molecular structures of compounds **1**, **2**, and **3**, showing the atom labelling schemes with displacement ellipsoids drawn at the 50% probability level and H atoms shown as small spheres of arbitrary radii

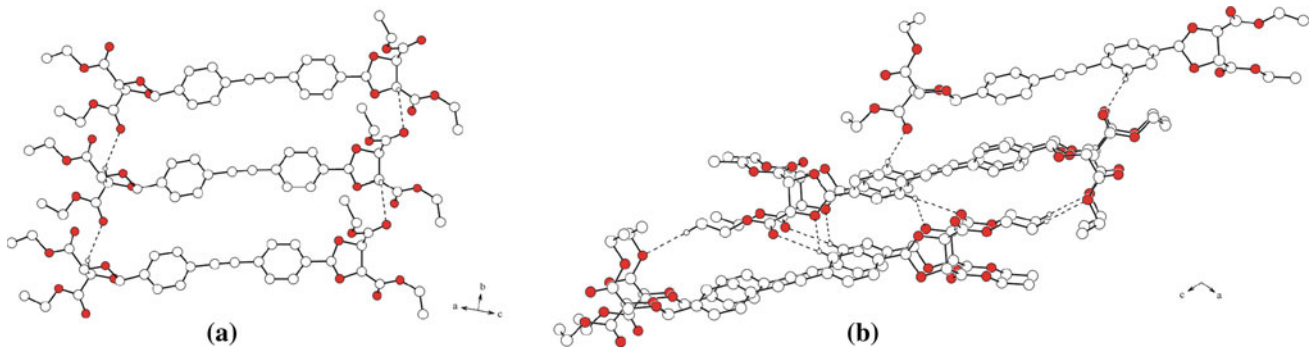

Fig. 4 Motifs of C–H···O hydrogen bonds within **a** and between **b** molecular chains of **1**. Intermolecular interactions are represented as *broken lines* and non-relevant H atoms are omitted for clarity

differences in the solid state. Of the five unique dioxolane moieties, only one adopts a twist conformation (dioxolane 1 of compound **1**), while the other four have an envelope conformation, which can be differentiated with regard to the flap atom. In case of the terminal alkyne **2**, both molecules contain dioxolane moieties where the chiral carbon atom C4 is out of plane. In contrast, C2 is not a part of the dioxolane plane in compounds **1** and **3**. A comparison with similarly substituted dioxolanes from the literature [13–16] shows that the envelope conformation of compound **2** with the chiral C-atom out of plane is rather rare.

Similarities and differences of the dioxolane units can be visualized by structural overlays (Mercury [39]). The overlay of all dioxolane ring atoms confirms that the dioxolane units of compounds **1** (Fig. 9a) and **2** (Fig. 9b), respectively, are rather similar. The graphical illustration also indicates that both dioxolane units of **1** are more similar than the classification (molecule 1: twist, molecule 2: envelope), based on the pucker parameters, suggests. Conformational differences between the dioxolane rings of compounds **1** and **3**, for example, are illustrated in Fig. 9c with a comparatively high standard deviation for the structure overlay (RMS = 0.192).

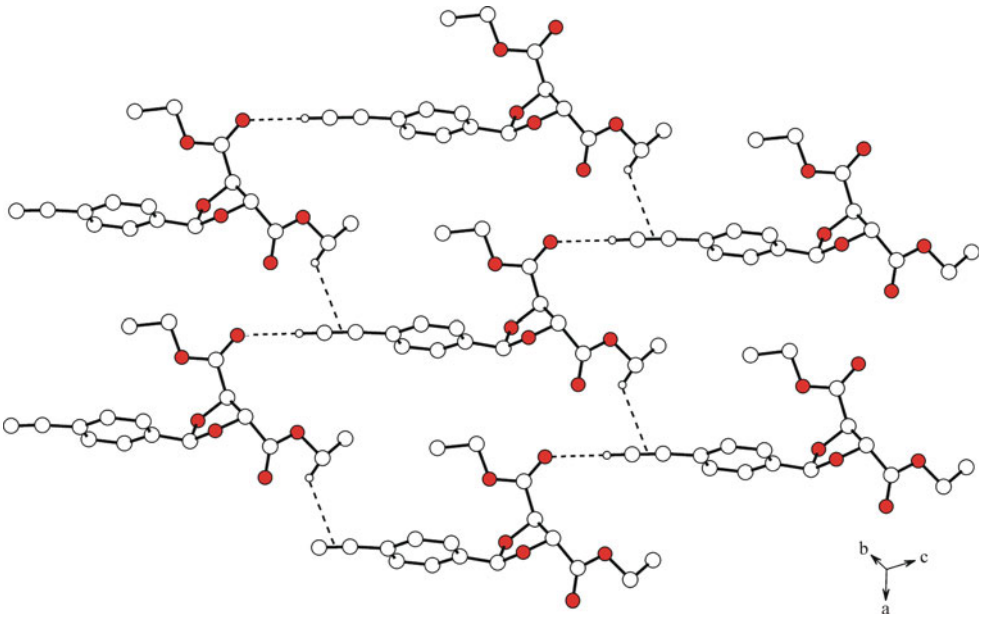

Fig. 5 Intermolecular interactions within one layer of molecules of **2** (*broken lines*). Non-relevant H atoms are omitted for clarity

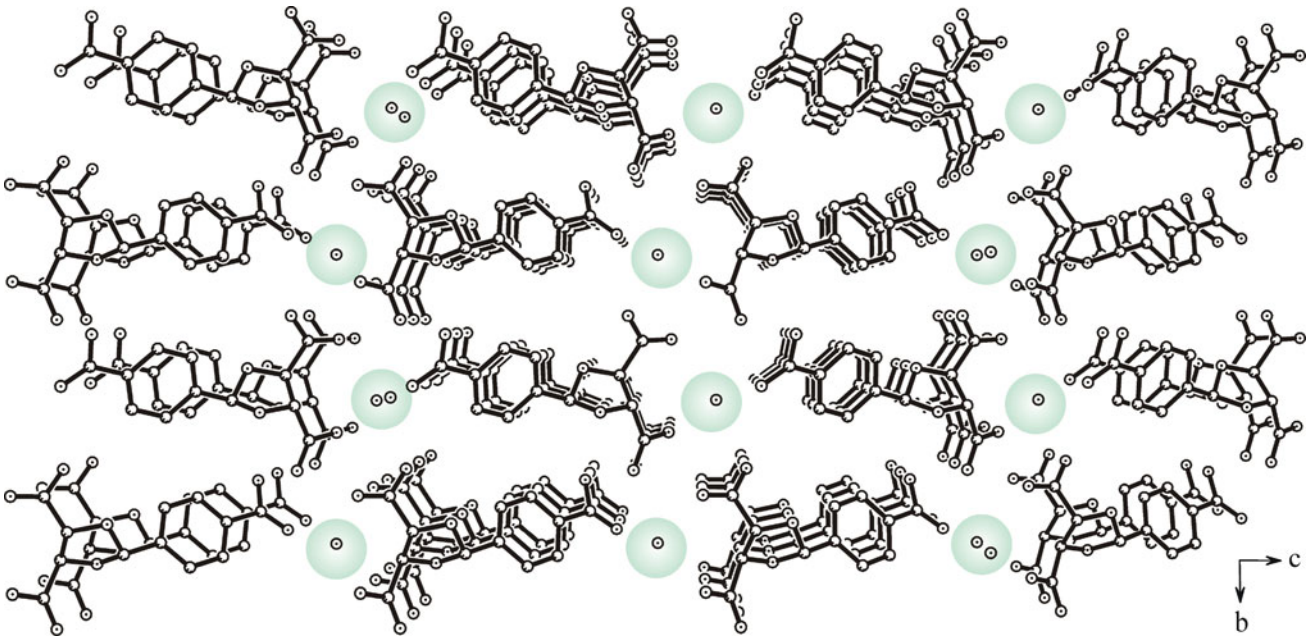

Fig. 6 Packing structure of compound **3** viewed along the *a* axis, showing molecular layers with enclosed crystal water (*highlighted*). H atoms are omitted for clarity

The stereochemistry of the molecules can also be described by the arrangement of dioxolane units with respect to the phenyl ring. Only the atoms of the dioxolane 2 of compound **1** and of the corresponding phenyl ring are almost coplanar, while the other four dioxolane units (dioxolane 1 of compound **1**, compounds **2** and **3**) are twisted relative to the plane of the aromatic spacer (Fig. 9d–f). The greatest deviation from planarity can be observed in case of dioxolane 1 (compound **1**) with an almost perpendicular alignment of dioxolane and phenyl moieties. By using enantiopure (4*R*,5*R*)-diethyl tartrate as a starting material, the stereochemistry is fixed and the substituents in position 4 and 5 of the dioxolane ring adopt a *trans* configuration. Nevertheless, there are significant

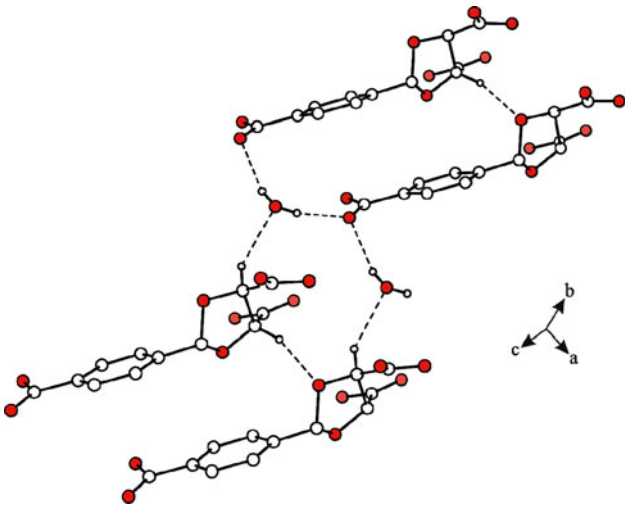

Fig. 7 Cyclic hydrogen bond network including **3** and H_2O molecules. Hydrogen bonds are represented as *broken lines*. Non-relevant H atoms are omitted for clarity

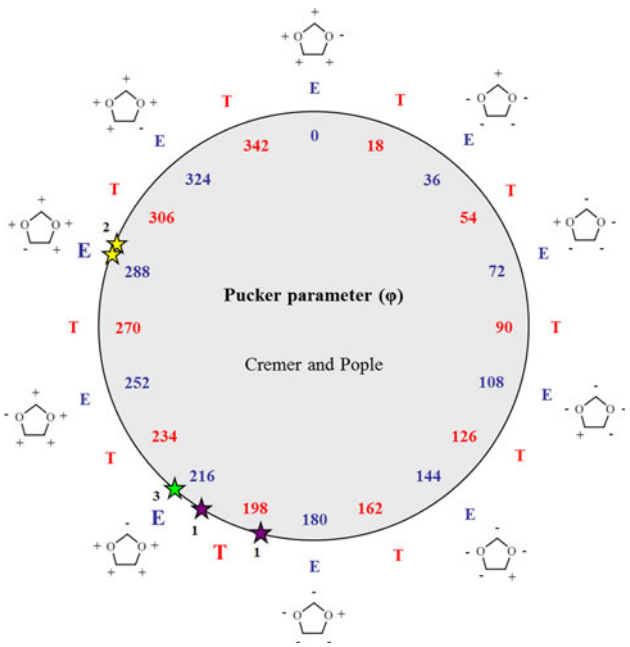

Fig. 8 Pseudorotation wheel of 1,3-dioxolane with notifications of corresponding pucker parameters of dioxolane units in the crystal structures of **1** (*purple*), **2** (*yellow*), and **3** (*green*) (color figure online)

differences concerning the alignment of ethoxycarbonyl and carboxy groups, respectively, with respect to the dioxolane moiety. This fact can be explained by sterical demands caused by the packing of molecules or by the different conformations of the dioxolane rings themselves. Figure 10 indicates that substituents in position 4 have a similar arrangement, while those in position 5 are twisted into different directions. The carbonyl oxygen atom is usually directed away from the dioxolane moiety, with the exception of the dioxolane ring 1 in compound **1**.

Conclusions

The new compounds (**1**–**3**) have been synthesized by applying a sequence of acetylenic protection, Pd-catalyzed coupling, deprotection, and transacetalization reactions involving L(+)-diethyl tartrate in the key transacetalization step. Using varying crystallization methods, solvent free structures of **1** and **2** and a hydrated crystal structure of **3** were obtained. While molecules of the tartaric ester derivative **1** are arranged in two-dimensional strands, compounds **2** and **3** adopt a layer structure. The data summarized in Table 2 permit a correlation between the strength/number of intermolecular interactions in the crystals and the melting points of the compounds. The solid phase structures of the esters **1** and **2** are exclusively stabilized by weak non-conventional hydrogen bonding comprising C–H···O and C–H···π(arene) type interactions which may explain the relatively low melting temperatures of 74–77 and 55–59 °C, respectively. In contrast, the presence of the water molecule in the hydrate **3** exerts a remarkable influence on the stability of the crystal, which is reflected by intense cross-linking of the crystal components, including the water molecule, via O–H···O hydrogen bonding, leading to a considerably enhanced melting point (203–206 °C). Thus, in a way, **3** deviates from the usual behavior of carboxylic acids forming a hydrogen bonded dimer motif of hydrogen bonds. Moreover, a comparison of all molecular structures revealed that the dioxolane ring adopts different conformations (twist and envelope isomers) even though the substitution pattern of this cyclic unit is similar in all three compounds.

Supplementary data

CCDC 839596 (**1**), 839597 (**2**) and 839598 (**3**·H_2O) contain the supplementary crystallographic data for this article. These data can be obtained free of charge at www.ccdc.com.ac.uk/retrieving.html [or from the Cambridge Crystallographic Data Centre (CCDC), 12 Union Road, Cambridge CB2 1EZ, UK; fax: +44(0)1223-336033; e-mail: deposit@ccdc.com.uk].

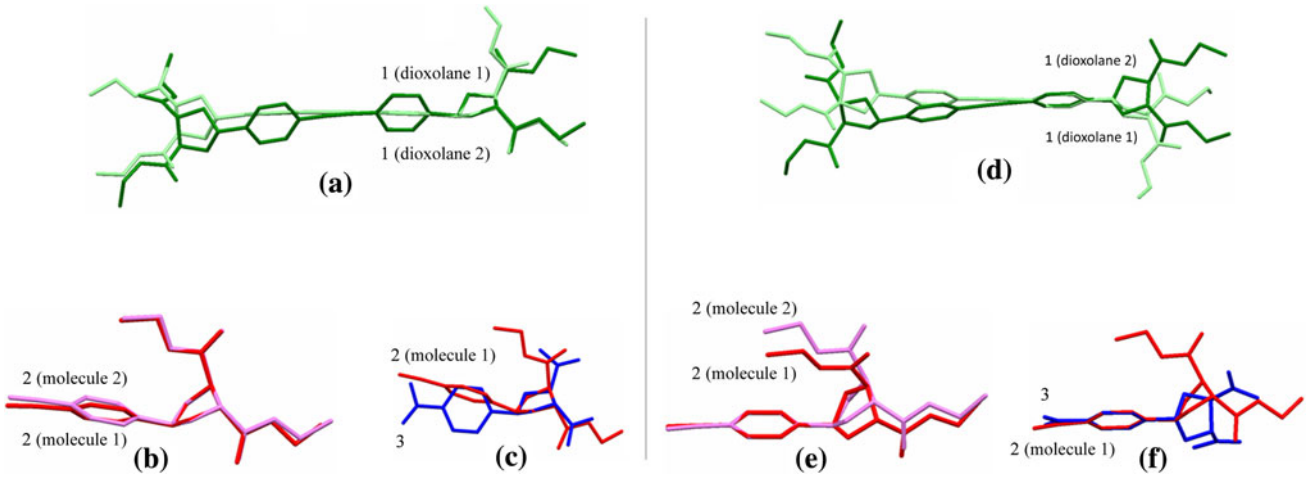

Fig. 9 Structural overlays of molecular fragments of **1** (*green* dioxolane 1, *light green* dioxolane 2), **2** (*red* molecule 1, *rose* molecule 2) and **3** (*blue*). Fitting of dioxolane ring atoms (**a**–**c**) and phenyl ring atoms (**d**–**f**). **a** RMS = 0.0402; **b** RMS = 0.0211; **c** RMS = 0.192; **d** RMS = 0.0598; **e** RMS = 0.0277; **f** RMS = 0.0339 (color figure online)

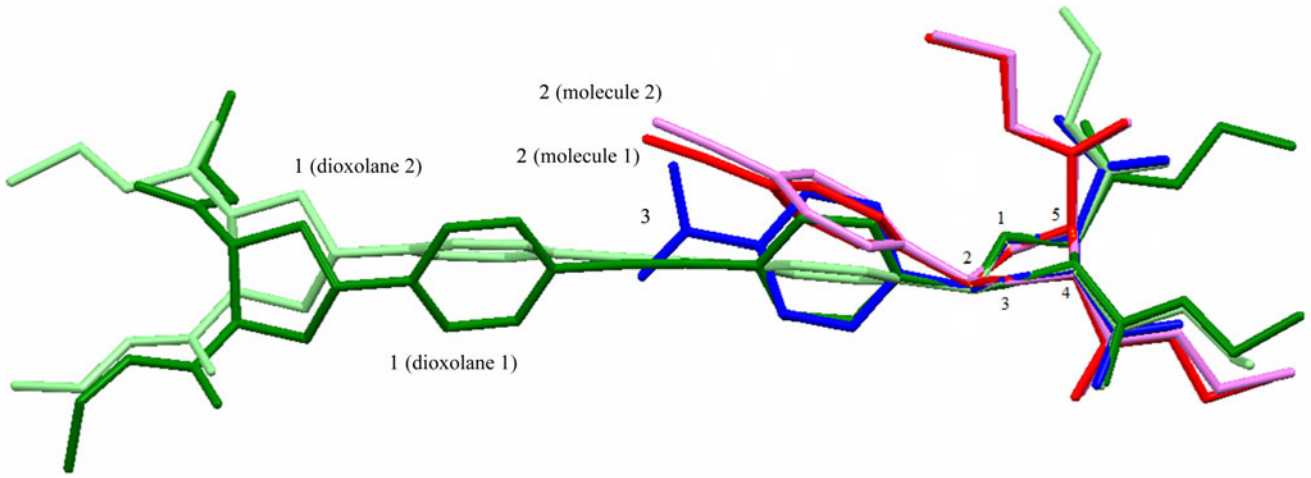

Fig. 10 Structural overlays of molecular fragments of **1** (*green* dioxolane 1, *light green* dioxolane 2), **2** (*red* molecule 1, *rose* molecule 2), and **3** (*blue*) by fitting dioxolane ring atoms (color figure online)

Acknowledgment Financial support from the Deutsche Forschungsgemeinschaft (DFG) under the program SPP 1362/1 is gratefully acknowledged.

References

1. Pasteur L (1848) C R Hebd Seances Acad Sci 26:535
2. Latscha HP, Linti GW, Klein HA (2004) Analytische Chemie. Springer, Berlin
3. Otto M (2006) Analytische Chemie. Wiley-VCH, Weinheim
4. Habermehl G, Hammann PE, Krebs HC, Ternes W (2008) Naturstoffchemie. Springer, Berlin
5. Seebach D, Beck AK, Heckel A (2001) Angew Chem 113:96
6. Zhong N, Zhao X, Ma H, Chen Y (2010) US Patent 007678 921B2
7. Kassai C, Juvancz Z, Balint J, Fogassy E, Kozma D (2000) Tetrahedron 56:42
8. Rosseinsky MJ (2004) Microporous Mesoporous Mater 73:15
9. Xu R, Pang W, Yu J, Huo Q, Chen J (2007) Chemistry of zeolithes and related porous materials. Wiley, Singapore
10. Kondo F, Iwaizumi T, Kimura H, Takeishi M (1997) Kobunshi Ronbunshu 54:908
11. Tuzuki Y (1939) Bull Chem Soc Jpn 14:19
12. Shim YJ, Choi K (2010) Org Lett 12:880
13. Li XH, Wang DC, Liu BN, Xu W (2008) Acta Crystallogr Sect E 64:2499
14. Liu HQ, Wang DC, Xu W, Yang Z, Gai T (2009) Acta Crystallogr Sect E 65:841
15. Belokon YN, Gagieva SC, Sukhova TA, Dmitriev AB, Lyssenko KA, Bravaya NM, Bulychev BM, Seebach D (2005) Russ Chem Bull 54:2384
16. Jiang J, Pan Y, Wang DC, Ou-yang PK (2007) Acta Crystallogr Sect E 63:1093
17. Kong SD, Luong A, Manorek G, Howell SB, Yang J (2007) Bioconjug Chem 18:293

18. Bruker (2007) SMART, SAINT, SHELXTL, SADABS. Bruker AXS Inc., Madison, WI
19. Sheldrick GM (2002) SADABS, Siemens Area Detector Absorption Correction Program. Universität Göttingen, Germany
20. Sheldrick GM (2008) Acta Crystallogr Sect A 64:112
21. Flack HD, Bernardinelli G (1999) Acta Crystallogr Sect A 55:908
22. Flack HD, Bernardinelli G (1999) J Appl Chem 33:1143
23. Spek AL (2009) Acta Crystallogr Sect D 65:148
24. Desiraju GR, Steiner T (1999) The weak hydrogen bond. Oxford University Press, Oxford, UK
25. Felsmann M, Eißmann F, Schwarzer A, Weber E (2011) Cryst Growth Des 11:982
26. Nishio M, Umezawa Y, Honda K, Tsuboyamad S, Suezawae H (2009) CrystEngComm 11:1757
27. Fischer C, Lin G, Bombicz P, Seichter W, Weber E (2011) Struct Chem 22:433
28. Boese R, Kirchner MT, Billups WE, Norman LR (2003) Angew Chem Int Ed 42:1961
29. Salonen LM, Ellermann M, Diederich F (2011) Angew Chem Int Ed 50:4808
30. Bernstein J, Novoa JJ, Boese R, Cirkel SA (2010) Chem Eur J 16:9047
31. Jeffrey GA (1997) An introduction to hydrogen bonding. Oxford University Press, Oxford, UK
32. Katzsch F, Eißmann D, Weber E (2011) Struct Chem. doi: 10.1007/s11224-011-9858-0]
33. Desiraju GR (1995) Angew Chem Int Ed 34:2311
34. Burrwos AD (2004) In: Mingos DMP (ed) Supramolecular assembly via hydrogen bonds I. Structure and bonding, vol 108. Springer, Berlin, pp 54–95
35. Cremer D, Pople JA (1975) J Am Chem Soc 97:1354
36. Lightner DA, Gurst JE (2000) Organic conformational analysis and stereochemistry from circular dichroism spectroscopy. Wiley, Chichester
37. Cros S, du Penhoa CH, Pérez S, Imberty A (1993) Carbohydr Res 248:81
38. Finch P (2010) Carbohydrates: structures, syntheses and dynamics. Kluwer, Dordrecht
39. Macrae CF, Bruno IJ, Chisholm JA, Edgington PR, McCabe P, Pidcock E, Rodriguez-Monge L, Taylor R, van de Streek J, Wood PA (2008) J Appl Crystallogr 41:466
40. Wang DC, Ge T, Wu WY, Xu W, Yang Z (2009) Acta Crystallogr Sect E 65:2230
41. Wang DC, Bai J, Xu W, Gai T, Liu HQ (2009) Acta Crystallogr Sect E 65:1960